Investigating Density Modelling with Neural Fields for Inverting Gravity Surveys

Daniel Wedge
Centre for Data-driven Geoscience, School of Earth and Oceans
The University of Western Australia
35 Stirling Hwy, Crawley WA 6009, Australia
daniel.wedge@uwa.edu.au

Abstract

In geophysics, gravity surveys measure variations in the gravitational field due to density anomalies in the Earth's crust. Inversion, i.e. *estimating the positions, extents, and densities of causative mass anomalies from the survey, is an ill-posed problem which has historically used voxel-based methods, with geological and geophysical constraints.*

We introduce a gravity survey inversion method utilising a neural field for predicting the class of relative density of a mass anomaly at given coordinates within a volume. The classes target the known densities of anomalies, ordered in increasing relative density allowing for ordinal regression. In training the network, the error in the predicted gravity response due to these anomalies, relative to the input gravity survey, is minimised.

Our initial investigations with synthetic data demonstrate that this neural field approach produces plausible density models consistent with the input gravity survey, and smooth density models are obtained in the presence of noise.

1. Introduction

Gravimetry is a field of geophysics whereby density variations in the Earth's crust are measured using a gravimeter. They are a widely used method for understanding the Earth's subsurface, for example for geological understanding of rock density distributions [6] and geological discontinuities [4]. Measurements can be post-processed to compensate for known variations *e.g.* due to the shape of the Earth, elevation above/below sea level, tides, and terrain [1]. Resampling to a regular grid simplifies visualisation of the data as a regular image and allows processing with filters such as for feature detection and upward continuation, *i.e.* calculating the gravity response at a higher elevation [1].

The gravitational response due to mass anomalies of known densities, locations, and extents can be calculated analytically [1], *i.e. forward modelling*. However, for the inverse problem, known as *inversion*, infinitely many distributions of causative masses can produce the observed response [6, 12]. For example, a single shallow mass, and larger or more dense deeper masses may produce equivalent responses. Approaches to counter this ambiguity include depth weighting [6], model pre-conditioning [12] and level set methods [4]. Constraints such as localising anomalies laterally [2]; bounds on thickness, density or maximum depth [10]; or restricting the inverted density values to a set of predetermined values [4] can improve inversions. Inversion methods have historically been voxel-based.

Some neural networks incorporate physical constraints in the loss functions. Cheng et al. [3] used a neural network approach to model the gravitational field around small bodies in space, *e.g.* asteroids, by predicting a gravitational force vector at coordinates relative to the asteroid; accurate knowledge of small bodies' variable gravitational fields is essential for trajectory computation for landing spacecraft on asteroids. Martin and Schaub used neural networks to map position to acceleration for space-borne measurements of gravitational fields of the Earth and Moon [7] and small bodies [8]. Izzo and Gómez [5] used a neural field to model a small body's shape and density distribution from orbiting spacecraft accelerations.

We introduce a method for inverting a gravity survey utilising a neural field for predicting the relative density at given coordinates within a volume. We train a multi-layer perceptron with sinusoidal activation functions [11] for ordinal regression of density class indices. The class index is mapped to a relative density value using a sum of sigmoids derived from the desired density value for each class; a gravity survey is forward modelled from the coordinates and predicted relative density values; the loss is calculated via comparison to the input gravity survey. A stratified sampling approach is used. The inverted volume contains smooth masses, which is generally preferable [6].

In this preliminary work, we apply the method to synthetic data in order to evaluate it against a known ground truth. The resultant density volumes accurately reproduce the input gravity survey in the presence of noise-corrupted

input data. The neural field representation provides for continuous density models, in contrast to classical voxel-based approaches and particularly at lower resolutions, and produces desirable smooth anomalies within the volume. These outcomes indicate that neural fields are suitable for density modelling in gravity survey inversion, and in the future may provide a framework for combining classical geophysical constraints with neural methods, for example, signed distance function methods are common to both fields.

Our approach operates on a single top-down gravity survey, in contrast to approaches for small body modelling [5, 7, 8] which use measurements from space probes orbiting a small body that provide 360° observations. In a computer vision analogy, our method is single view 3D reconstruction, compared to 3D reconstruction from viewing rays surrounding the object in all three dimensions. Also, for small body modelling the total mass is known, whereas in our application it is not. Hence our method tackles problems not present in small body modelling.

2. Method

A multi-layer perceptron with sinusoidal activation functions [11] regresses a relative density class index $c_{(x,y,z)}$ from input coordinates (x, y, z), using 3 hidden layers of 128 features each. The class index is used to calculate a relative density value. Let $\boldsymbol{\rho} = \{\rho_1, \ldots, \rho_N\}$, where $\rho_i < \rho_{i+1}$, represent the densities of specific mineralogies or fluids, relative to the geological background density which is represened by a class with relative density of 0. Negative relative densities represent less dense material or voids. This use of specific densities follows existing inversion methods [4]. Ideally, $c_{(x,y,z)} \in \{1, \ldots, N\}$, specifying a particular relative density $\rho_{c_{(x,y,z)}} \in \boldsymbol{\rho}$ at (x, y, z). However as the regressed density class index is real-valued, we use a sum of sigmoids to calculate a relative density as shown in Fig. 1. This resulting relative density function is continuous, and is guided toward the specific desired ordered values in $\boldsymbol{\rho}$. Successive sigmoids are translated by 1, and scaled by the difference in successive relative densities. We use $S = 25$ for steeper transitions; the offset of 0.5 translates the inflection points to halfway between integer class indices. The predicted mass anomaly m at (x, y, z) is computed from the class index and density values:

$$m(x, y, z) = \rho_1 + \sum_{n \in [2,N]} \frac{\rho_n - \rho_{n-1}}{1 + e^{-(c_{(x,y,z)} - n + 0.5) \times S}} \quad (1)$$

For masses m in the modelled volume of interest V, the vertical component g_z of the gravitational potential field at a given survey location (x_s, y_s, z_s) is calculated via [1]:

$$g_z(x_s, y_s, z_s) = -G \sum_{(x,y,z) \in V} m(x, y, z) \frac{(z_s - z)}{r^3}, \quad (2)$$

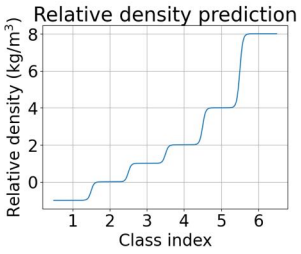

Figure 1. The relative density is calculated from the class index using a sum of sigmoids.

where G is the gravitational constant, and

$$r = \sqrt{(x_s - x)^2 + (y_s - y)^2 + (z_s - z)^2}. \quad (3)$$

In practice, coordinates in each dimension are normalised to $[-1, 1]$ before being input to the MLP to predict the density class index, which is similarly normalised.

In training, the volume is sampled to predict the relative density throughout. A stratified sampling method [9] samples the volume at two scales: regularly at a larger scale and then stochastically within each larger scale unit. These finer scale coordinates and their predicted relative densities are used to forward model a predicted gravitational response. Since this approach sub-samples the volume, at each location a point mass representive of a cube with the larger scale's side length and the predicted density is forward modelled, to simulate it being volumetrically representative of a sample at the larger scale. We hypothesize that this sampling approach is particularly suited for this application where smooth inversion volumes are desirable. The forward model is computed at x_s and y_s values covering the survey's lateral extent, while the survey elevation z_s is constant. The training loss is then the mean squared error between the observed response in the input gravity survey, and this predicted forward modelled gravitational response.

3. Results

We present results for inverting a gravity survey forward modelled from five synthetic spherical masses of various densities, sizes, and depths listed in Tab. 1, located in a $2048 \times 2048 \times 2048$m cube. The gravimetry responses are reported in milligals, where 1 Gal = 1 cm s^{-2}. For numerical simplicity we used $G = 0.1$ N m^2 kg^{-2} in forward modelling. Stratified sampling first sampled the volume in $32 \times 32 \times 32$m voxels, then stochastically within each voxel. The survey resolution is 512×512, with a survey elevation of $z_s = 400$m. The model uses relative density values $\boldsymbol{\rho} = \{-1, 0, 1, 2, 4, 8\}$ kg/m^3. A PyTorch implementation used the Adam optimiser with an initial learning rate of 1×10^{-4}, and trained for 5000 iterations.

Fig. 2 shows slices of the inverted continuous density volumes, examining its sensitivity to the initial conditions.

Mass ID	x m	y m	z m	Radius m	Rel. density kg/m^3
A	512	1536	384	100	4
B	1536	1024	256	100	2
C	1024	256	64	64	2
D	1536	1536	128	90	1
E	512	512	768	90	-1

Table 1. The synthetic masses' relative densities, radii, and locations in a $2048 \times 2048 \times 2048$m volume.

As inversion is an ill-posed problem, the initial conditions influence the final inversion volume. The network was initialised by training it with the known class index for each (x, y, z) coordinate as per Tab. 1 and the variations described below. The resulting volumes are plausible and the predicted g_z forward models are highly similar to the target gravity survey response, indicating that neural fields are capable of numerically accurate inversion. The ground truth masses are shown in (a). Volume (b) is initialised to all zeros, and the method produces large, shallow, low density masses, laterally located over the corresponding ground truth masses of higher density and producing similar gravitational responses. Volume (c) is initialised with masses with double the densities at half the depth and omitting mass E; remnants of this double-density initialisation are visible for masses C (at 64m), D (also 64m) and B (128m), with larger, smooth, low density masses added contributing to the desired gravitational response. In (d), half-density masses at double the depth are modelled and mass E omitted; here the desired response is modelled with larger, deeper masses, with particular reference to the equivalent of mass A being largely modelled at 768m. Volumes (e) and (f) are initialised with 3 masses roughly at the positions of A, B and D but with positions and radii perturbed so that the initial masses are not representative of the ground truth; additionally, Gaussian noise with $\sigma = 3$ mGal is added to the input g_z survey in (f). In these cases we note qualitatively similar and smooth volumes are obtained despite the added measurement noise, and the initialisation of deeper masses A and B influences the inversion.

This preliminary study shows that the method accurately models the input g_z survey with masses of homogenous density, though we note a bias toward larger, lower density masses. Some deeper, low-density masses cover a large lateral area, but do not significantly contribute to the forward modelled g_z due to their depth and density. We anticipate incorporating classical geophysical regularization methods to address these biases. The negative relative density class is used sparingly and is not used to cancel out responses from positive density anomalies. We hypothesise that stratified sampling provides spatial regularization to produce smooth results, and will investigate this in future work.

4. Conclusions

We have introduced a novel framework to invert gravity surveys, utilising an neural field to model the underlying density class indices within a volume; the indices are then mapped to desired relative density values. Our initial investigations demonstrate that the method produces smooth models, even with added noise, with the forward modelled results highly similar to the input gravity survey. As with existing methods, the inversion results are dependent on the quality of the provided depth and density estimates. Future work will apply classical geophysical and geological priors and regularization approaches to improve depth estimates and compactness within this framework, and apply the method to more complex scenarios and real-world data.

References

[1] Richard J. Blakely. *Potential Theory in Gravity & Magnetic Applications*. Cambridge University Press, 1995. 1, 2

[2] Richard J. Blakely and Robert W. Simpson. Approximating edges of source bodies from magnetic or gravity anomalies. *Geophysics*, 51(7):1494–1498, 1986. 1

[3] Lin Cheng, Zhenbo Wang, Yo Song, and Fanghua Jiang. Real-time optimal control for irregular asteroid landings using deep neural networks. *Acta Astronautica*, 170:66–79, 2020. 1

[4] Jérémie Giraud, Mark Lindsay, and Mark Jessell. Generalization of level-set inversion to an arbitrary number of geologic units in a regularized least-squares framework. *Geophysics*, 86(4), 2021. 1, 2

[5] Dario Izzo and Pablo Gómez. Geodesy of irregular small bodies via neural density fields. *Communications Engineering*, 1(1):48, 2022. 1, 2

[6] Yaoguo Li and Douglas W. Oldenburg. 3-D inversion of gravity data. *Geophysics*, 63(1):109–119, 1998. 1

[7] John Martin and Hanspeter Schaub. Physics-informed neural networks for gravity field modeling of the Earth and Moon. *Celestial Mechanics and Dynamical Astronomy*, 2022. 1, 2

[8] John Martin and Hanspeter Schaub. Physics-informed neural networks for gravity field modeling of small bodies. *Celestial Mechanics and Dynamical Astronomy*, 2022. 1, 2

[9] Ben Mildenhall, Pratul P. Srinivasan, Matthew Tancik, Jonathan T. Barron, Ravi Ramamoorthi, and Ren Ng. NeRF: Representing scenes as neural radiance fields for view synthesis. In *Proceedings of the European Conference on Computer Vision*, 2020. 2

[10] Robert L. Parker. The theory of ideal bodies for gravity interpretation. *Geophysical Journal of the Royal Astronomical Society*, 42:315–334, 1975. 1

[11] Vincent Sitzmann, Julien Martel, Alexander Bergman, David Lindell, and Gordon Wetzstein. Implicit neural representations with periodic activation functions. *Proceedings of the 34th International Conference on Neural Information Processing Systems*, pages 7462–7473, 2020. 1, 2

[12] Michael S. Zhdanov. *Inverse Theory and Applications in Geophysics (2nd Edition)*. Elsevier, 1995. 1

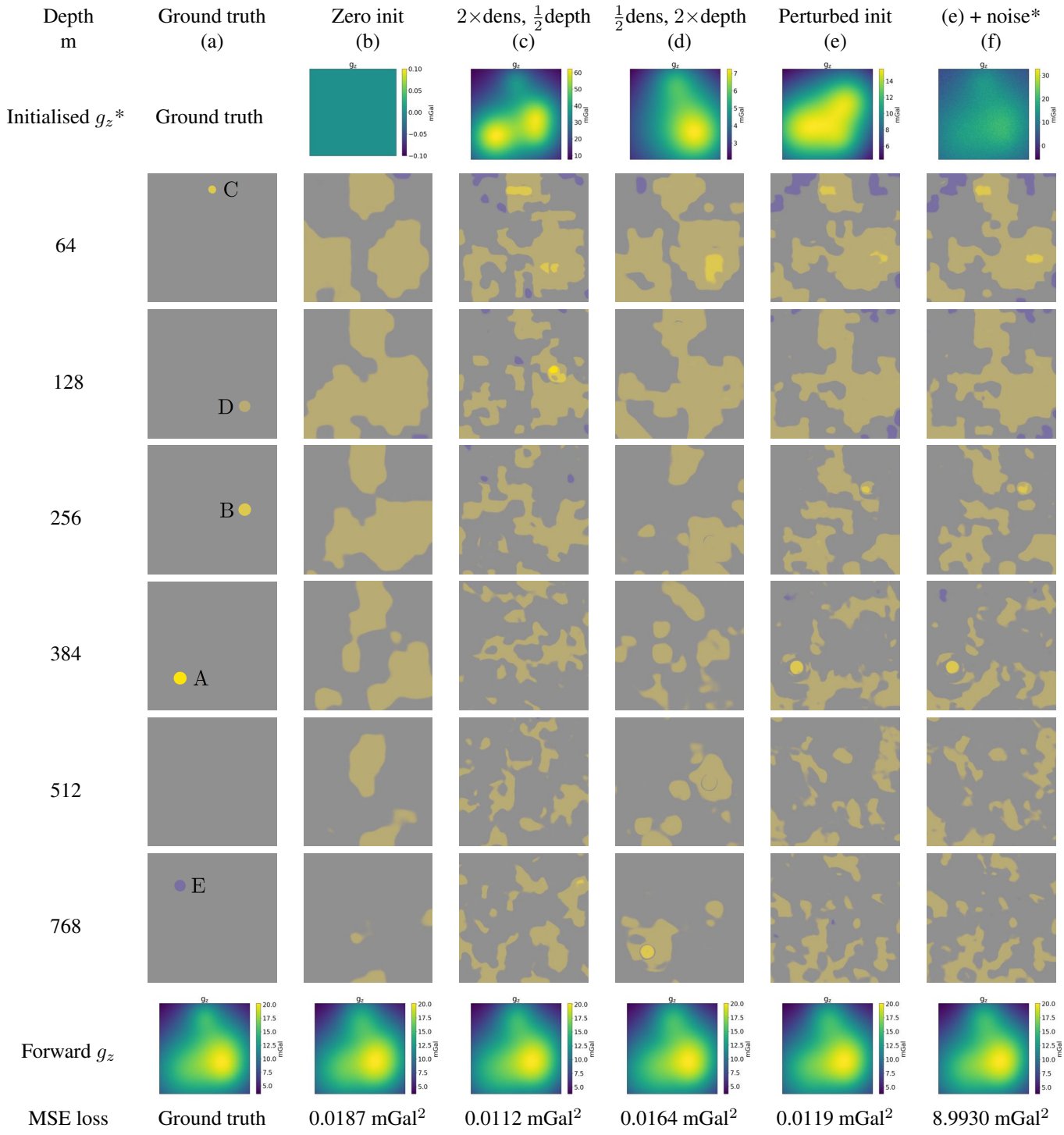

Figure 2. Inversion results due to different initialisations. Rows illustrate: the volume's forward modelled g_z after initialisation (* except for (f) the noise-corrupted target g_z is shown instead, note the initial g_z is the same as (e)); depth slices of the inverted volume; the forward modelled g_z response due to the inverted volume; and the final loss relative to the ground truth g_z. Columns contain: (a) Annotated ground truth masses listed in Tab. 1. The origin is in the top-left corner. Then, inversion results with: (b) relative density initialised to 0 everywhere; (d) initialisation based on double density spheres at half depth; (d) half density spheres at double depth; (e) perturbed locations, sizes and missing masses; (f) as per (e), with added Gaussian noise of 3 mGal, which contributes to the larger loss. For depth slices, blue/grey/yellow indicates negative/0/positive relative density compared to the background; saturation increases with magnitude of relative density. Compare colours in (a) to Tab. 1 for relative density values. Please refer to a digital version of the manuscript to view the figure in more detail.